TÜBİTAK

Turkish Journal of Earth Sciences

http://journals.tubitak.gov.tr/earth/

Research Article

Turkish J Earth Sci
(2015) 24: 365-382

doi:10.3906/yer-1412-30

Rare earth element geochemistry of the Upper Permian limestone: the Kanigorgeh mining district, NW Iran

Ali ABEDINI[1,*], Ali Asghar CALAGARI[2]

[1]Department of Geology, Faculty of Sciences, Urmia University, Urmia, Iran

[2]Department of Earth Sciences, Faculty of Natural Sciences, Tabriz University, Tabriz, Iran

Received: 26.12.2014 • **Accepted/Published Online:** 02.05.2015 • **Printed:** 30.06.2015

Abstract: The limestone of the Ruteh Formation of Upper Permian age in the Kanigorgeh district (northeast of Bukan, NW Iran) contains several layers and lenses of bauxitic ores. Mineralogical data show that this limestone consists of calcite and quartz as major and plagioclase, kaolinite, and hematite as minor mineral phases. Geochemical analyses reveal that the proportions of ΣREEs (La-Lu) in this limestone vary from 35.28 to 160.78 ppm. The values of Eu and Ce anomalies (normalized to PAAS) of the limestone have ranges of 1.11–1.68 and 0.89–1.16, respectively. The high values of ΣREEs; low values of Y/Ho; strong and positive correlations between ΣREEs and elements such as Si, Al, Ti, V, Co, Ni, Rb, Cu, and Nb; and negative correlations between CaO and ΣREEs suggest that the observed variations in values of ΣREEs in the limestone were controlled principally by the quantity of detrital materials. Geochemical data also illustrate that the observed positive Eu anomalies in the limestone may be due to the presence of plagioclase and also a function of diagenetic processes. Furthermore, the variations in Ce anomalies may be due to the detrital input. The distribution of REEs (normalized to chondrite) illustrates different patterns in both rocks (the limestone and the bauxitic ores) in light of differentiation degree of LREEs from HREEs and values of conservative indexes such as Eu anomaly. Considering these pronounced discrepancies, it appears that the limestone, despite having relatively high concentration of ΣREEs, did not play a significant role in supplying lanthanides for the bauxitic ores.

Key words: Rare earth elements, geochemistry, limestone, Ruteh Formation, Kanigorgeh, Iran

1. Introduction

During the past few decades, the behavior and mode of distribution of rare earth elements (REEs) in carbonate rocks were extensively investigated by many researchers (Elderfield et al., 1990; Armstrong-Altrin et al., 2003; Nothdurft et al., 2004; Madhavaraju and Lee, 2009; Madhavaraju et al., 2010; Nagarajan et al., 2011; Nagendra et al., 2011; Madhavaraju and González-León, 2012; Song et al., 2014). The studies done showed that the important factors influencing enrichment and depletion of REEs in carbonate rocks are 1) the amounts of detrital materials of terrigenous origin (Piper, 1974; McLennan, 1989; Nagarajan et al., 2011), 2) the variation in oxygen level of seawater (Liu et al., 1988), 3) the proximity to area of origin (Murray et al., 1991b), 4) biogenic deposition from seawater (Murphy and Dymond, 1984), 5) the variation in surface productivity (Toyoda et al., 1990), 6) the lithology and diagenesis (Madhavaraju and Ramasamy, 1999), and 7) scavenging processes related to depth, salinity, and oxygen level of seawater (Greaves et al., 1999). The results of recent investigations revealed that geochemical studies on REEs in carbonate rocks furnish a suitable basis for reconstruction of paleogeographic conditions (Madhavaraju and González-León, 2012).

The Ruteh Formation (Upper Permian) is very widespread in the northwest of Iran and includes limestone and dolomite. There is a distinct coexistence between the units of this Formation and certain horizons of lateritic-bauxitic ores (Abedini and Calagari, 2013a, 2013b). In the study area, the formation acted as either host or bedrock in different places for these residual deposits. The Kanigorgeh mining district is a typical area rich in bauxitic materials in NW Iran. There are two distinct bauxitic horizons in the district. The first one, whose ores are Ti-rich, belongs to the Upper Permian, and the second one has Fe-rich ores of Permo-Triassic age. The mineralogical and geochemical features of both horizons were investigated in detail by Abedini and Calagari (2013c, 2014). In both studies, based upon a series of geochemical parameters such as calculation of accumulation coefficients of trace elements; concentration values of some major and trace elements like Al, Ti, Fe, Mn, Si, Cr, Ni, and Nb; and elemental

* Correspondence: a.abedini@urmia.ac.ir

ratios such as Zr/Ti and Nb/Y, the principal source of the bauxitic layers and lenses in the Kanigorgeh district was recognized to be mafic igneous rocks, mainly with basaltic composition. The relicts of such rocks are still present at the contact of the bauxitic ores and the host limestone. So far, no geochemical studies on carbonate rocks of the Ruteh Formation have been carried out. Geochemical considerations of REEs in the limestone of the Ruteh Formation could be important in two respects. First, geochemical investigation can greatly contribute to determining how much the limestone (as host rock) might have the capacity to provide REEs for the bauxitic ores. In recent studies implemented by Liu et al. (2010), it was specified that in bauxitic ores associated with carbonate host rocks in addition to igneous rocks, which can furnish most of the major and trace elements for residual ores, the host limestone could also play a crucial role in supplying some of the ore constituents, especially REEs. Second, determination of the source of REEs in limestone not only can help to establish the source of REEs in the layers and lenses of the studied bauxitic ores in the Kanigorgeh district but also can furnish very useful information on factors involved in distribution of REEs in both the limestone (host rock) and the bauxitic ores. By regarding these premises, in this study, with reliance on mineralogical and geochemical considerations, we have endeavored to present comprehensive information on the source of REEs as well as the reasons for occurrence of Eu and Ce anomalies in the limestone of the Ruteh Formation, and also to determine the potential portion of contribution of this rock in light of providing REEs for the bauxitic ores in Kanigorgeh district.

2. Geological setting

The Bukan basin is underlain mainly by Paleozoic and Infra-Cambrian sedimentary sequences. These rocks show fairly continuous succession, but there is a stratigraphic gap from the Silurian to the Carboniferous so that the Permian sediments overlie unconformably on Ordovician and older basement rocks. The sedimentation of the limestone was interrupted by several epeirogenic movements in the uppermost Permian. The surface expression of this limestone displays karstic erosion, which may be recognizable by the presence of volcanic lavas and bauxitic-lateritic lenses (Kamineni and Efthekhar-Nezhad, 1977; Calagari and Abedini, 2007; Abedini and Calagari, 2013a, 2013b, 2013c; Calagari et al., 2010, 2015). The carbonates of the Ruteh Formation are believed to be the second Permian sedimentary cycle in the Bukan basin. In most parts of this basin, the Ruteh Formation consists of gray to dark gray massive to layered limestone and dolomite with thin interlayered marl. Aghanabati (2004) reported that the depositional environment of the Ruteh Formation is similar to modern carbonate-depositing environments, especially along the southern coasts of the Persian Gulf.

The Kanigorgeh bauxite-bearing district is located ~20 km northeast of Bukan, West Azarbaidjan Province, NW Iran. According to the structural divisions of Iran it is a part of the Khoy-Mahabad zone (Abedini and Calagari, 2014) (Figure 1a). The oldest lithologic units in the area are sandstone and shale of the Dorud Formation (Lower Permian) overlain by dolomite and limestone of the Ruteh Formation (Upper Permian). The Ruteh Formation contains considerable outcrops of lateritic-bauxitic materials in NW Iran. Geologic characteristics of bauxites in this area were considered in detail by Abedini and Calagari (2013c, 2014).

In a type section (~450 m thick) in this mining district, the Ruteh Formation consists mainly of four lithologic units: 1) thin-layered dolomite, 2) medium- to thick-layered dolomitic limestone, 3) medium- to thick-layered limestone containing nodules and bands of chert, and 4) medium-layered dolomitic limestone (Figure 2). The limestone unit is gray and fossiliferous with a micritic nature. According to the existing fossils of corals, brachiopods, algae, and foraminifera within this formation, its age was attributed to the lower part of the Upper Permian (Thuringian) (Aghanabati, 2004).

The depositional cessation can be distinguished by the presence of horizons of Ti-rich and Fe-rich bauxitic ores in this limestone. Silicification, brecciation, and intense shearing are the interesting geological aspects of this limestone.

The limestone is unconformably overlain by dolomites of the Elika Formation of Triassic age (Abedini and Calagari, 2014). The stratigraphic sequence in the area is followed by Cretaceous units (sandstone, shale, conglomerate, and limestone), and carbonate rocks of the Qom Formation (Miocene) and Quaternary alluvial sediments (Figure 1b).

3. Methodology

The sampling was done on a 450-m-thick selective profile of the Ruteh Formation with intervals of 3–25 m. Eighty rock samples were collected. After microscopic examinations, 15 representative samples of the limestone were chosen for chemical analyses. The selected samples first were washed by distilled water to remove contamination and then were air-dried and ground in a tungsten carbide mortar. The ground samples were sieved through a 200 ASTM mesh. Prepared samples (0.2 g) were added to lithium metaborate/lithium tetraborate flux (0.9 g), mixed well, and fused in a furnace at 1000 °C. The resulting melt was then cooled and dissolved in 100 mL of 4% nitric acid/2% hydrochloric acid. These solutions were then analyzed for major elements by using inductively coupled plasma-atomic emission spectrometry (ICP-AES) and for trace

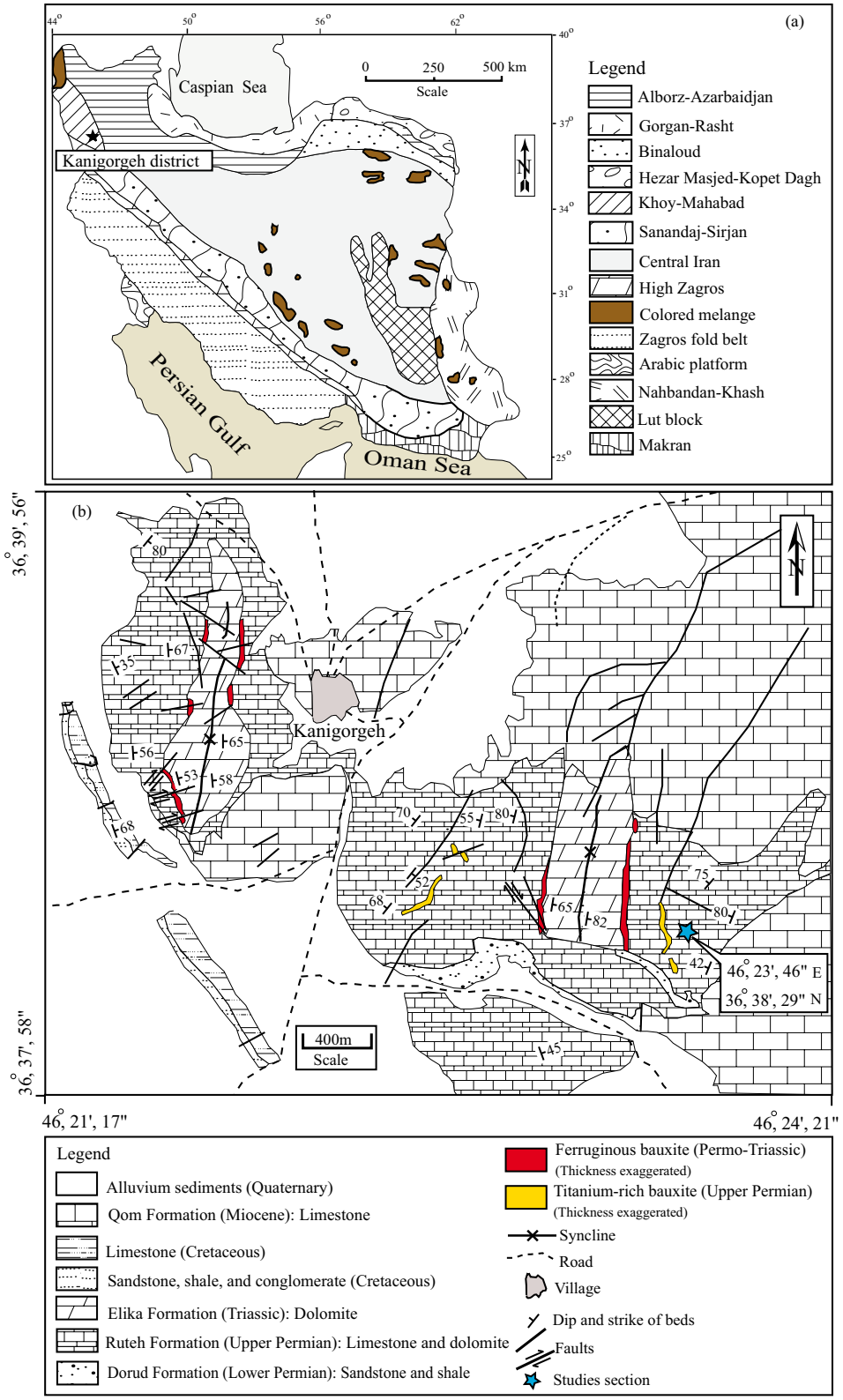

Figure 1. (a) Position of the Kanigorgeh mining district on the index structural map of Iran. **(b)** Geologic map of the studied area on which the position of the Ruteh Formation is shown (Abedini and Calagari, 2014).

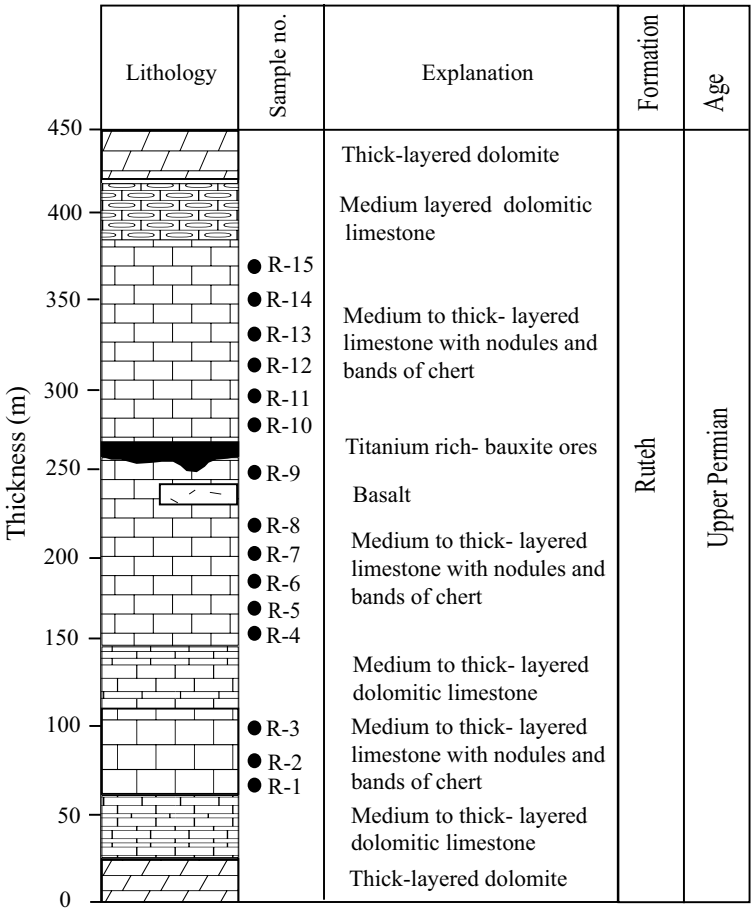

Figure 2. Lithostratigraphic section of the Ruteh Formation at Kanigorgeh showing the locations of collected samples. The filled circles show the position of analyzed samples used for geochemical considerations.

and rare earth elements by inductively coupled plasma-mass spectrometry (ICP-MS) methods in the laboratories of ALS Chemex, Canada (see Table 1). The loss on ignition (LOI) values of these samples were measured by weight reduction of 1 g of the sample after 90 min of heating at 950 °C. The detection limits for major oxides were about 0.01 wt.%, for trace elements within the range of 0.04–10 ppm, and for rare earth elements within the range of 0.01–0.5 ppm.

For determination of the major rock-forming minerals in the limestone, 7 samples were randomly selected for X-ray diffraction (XRD) analysis using a Siemens model D-5000 diffractometer with CuKα radiation, graphite monochromator, voltage of 40 kV, beam current of 80 mA, continuous scanning, scanning speed of 8°/min, scan range of 2°–70°, slit DS = SS = 1°, ambient temperature of 18 °C, and humidity of 30% in the facilities of the Geological Survey of Iran.

In the present study, for better interpretation, attempts were made to calculate the Pearson correlation coefficients among elements (Rollinson, 1993) with SPSS 16. For calculation of Eu and Ce anomalies, the corresponding values were normalized to post-Archean Australian shale (PAAS) by using the following formulas (Taylor and McLennan, 1985):

$$Eu/Eu^{*} = Eu_N / [(Sm_N \times Gd_N)]^{1/2},$$
$$Ce/Ce^{*} = 2Ce_N / (La_N + Pr_N),$$

where N stands for the normalization of REEs to PAAS.

4. Results

The XRD results show that the limestone consists of calcite, quartz, plagioclase, kaolinite, and hematite in rock-forming quantities (Figures 3a and 3b).

Concentration values of major, trace, and rare earth elements in samples of the limestone are listed in Table

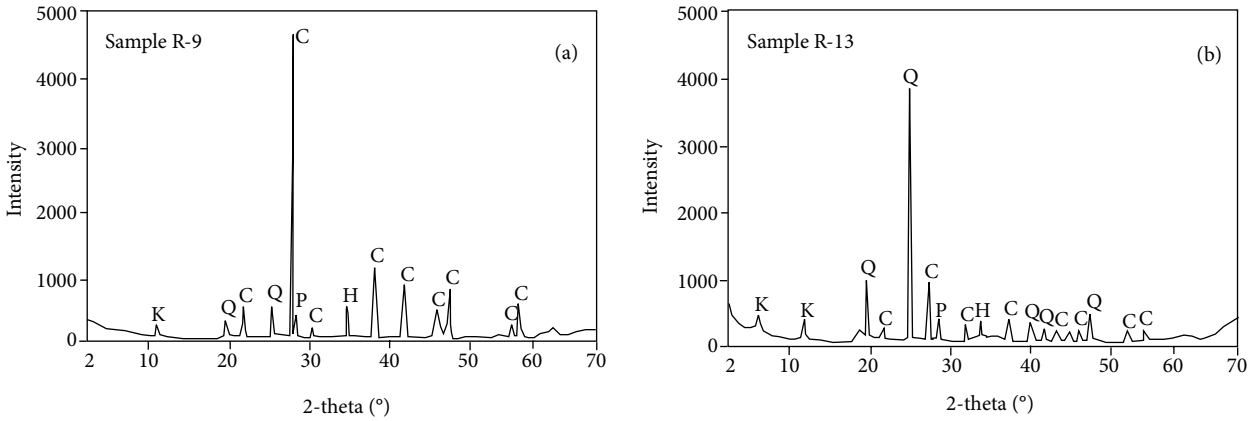

Figure 3. Patterns of XRD analyses for 2 typical samples from the limestone at Kanigorgeh. K: Kaolinite, C: calcite, Q: quartz, P: plagioclase, and H: hematite.

1. Illustration of bivariate plots between pairs of major elements (see data in Table 1) show that correlation coefficients are strong and positive for Al_2O_3 – SiO_2 (r = 0.97; Figure 4a), weak and negative for Fe_2O_3 – SiO_2 (r = –0.38; Figure 4b), weak and negative for Al_2O_3 – CaO (r = –0.38; Figure 4c), weak and positive for Fe_2O_3 – CaO (r = 0.28; Figure 4d), strong and positive for Al_2O_3 – TiO_2 (r = 0.95; Figure 4e), weak and negative for Fe_2O_3 – TiO_2 (r = –0.46; Figure 4f), weak and negative for SiO_2 – CaO (r = –0.36; Figure 4g), and strong and positive for TiO_2 – SiO_2 (r = 0.97; Figure 4h). What can be deduced from these graphs is that CaO, compared with other constituent oxides of the limestone, has a totally different origin. In comparison with marine carbonate (Turekian and Wedepohl, 1961), the samples of the studied limestone show weak depletion along with strong enrichment for elements such as V, Cr, Ni, and Rb; strong depletion for elements like Sr and Y; and notable enrichment for elements like Co, Cu, Rb, Zr, Nb, Ba, and Hf (Figure 5).

The ΣREE values in the studied limestone have a range of 35.28–160.78 ppm. In comparison with the typical marine carbonate (Bellanca et al., 1997), these values display both depletion and enrichment trends (Figure 6). The values of Eu/Eu* and Ce/Ce* have ranges of 1.11–1.68 and 0.89–1.16, respectively. The ΣREEs, in general, have positive correlations with certain major and trace elements such as Si, Ti, V, Co, Ni, Rb, and Nb (Table 2). The values of Eu/Eu* and Ce/Ce* have ranges of 1.11–1.68 and 0.89–1.16, respectively. The values of Er/Nd and Y/Ho are also within the range of 0.04–0.05 and 3.99–61.61, respectively. The ΣREEs, in general, have positive correlations with certain major and trace elements such as Si, Ti, V, Co, Ni, Rb, and Nb (Table 2).

5. Discussion

5.1. The source of REEs in the limestone

Commonly, the distribution pattern of REEs in limestones and bauxites can have occurred due to factors such as incorporation of terrigenous materials (Elderfield et al., 1990; Hanilçi, 2013), of Mn and Fe oxides (e.g., Bau et al., 1996), and of phosphates (e.g., Byrne et al., 1996). The negative correlations between REEs and Fe_2O_3 (r = –0.40) and the lack of notable positive correlation between MnO and phosphates (r = 0.38) will rule out the likelihood of significant contamination generated by Mn and Fe oxides in the limestone.

The strong and positive correlation between REEs and phosphates (r = 0.98; Figure 7a) depicts that in addition to terrigenous origin for REEs in the limestone, the diagenetic fluids also had an effective role in supplying REEs.

The concentration of Al_2O_3 in limestones is closely related to clay content. Therefore, Al_2O_3 concentration is considered as a proxy for shale contamination (Northdurft et al., 2004). The mean analytical value of Al_2O_3 in the limestone at Kanigorgeh is ~4.45 wt.%, which is far greater than the average values of siliciclastic-contaminated limestones (0.42 wt.%; Veizer, 1983). This concentration value shows strong and positive correlation with the ΣREE content (r = 0.94; Figure 7b), suggesting an intense contamination (Madhavaraju et al., 2010).

Recent investigations showed that distinguishing the terrigenous source for REEs in limestones is possible by considering the correlation coefficients between REEs and certain major and trace elements. Commonly, REEs with detrital origin have positive correlations with elements such as Si, Ti, Al, K, Sc, Cr, Co, Rb, Y, V, Ni, and Nb, and negative correlation with CaO (Madhavaraju et al., 2010; Nagarajan et al., 2011; Nagendra et al., 2011). Consideration of correlation coefficients between elements

Table 1. A list of whole-rock chemical analyses of samples taken from the limestone at Kanigorgeh.

	R-1	R-2	R-3	R-4	R-5	R-6	R-7	R-8
SiO_2 (wt.%)	15.21	15.51	12.41	14.03	14.64	15.82	11.12	14.99
Al_2O_3	6.08	6.25	4.96	5.51	5.74	5.33	4.15	5.41
Fe_2O_3	1.39	2.03	2.18	1.51	1.84	1.35	1.92	1.51
CaO	42.51	42.56	42.57	42.68	42.56	42.84	42.64	42.65
MgO	0.79	0.79	0.84	0.78	0.79	0.82	0.79	0.74
Na_2O	0.03	0.06	0.09	0.04	0.06	0.03	0.04	0.03
K_2O	0.69	0.82	0.68	0.55	0.81	0.28	0.54	0.71
TiO_2	0.15	0.11	0.07	0.11	0.12	0.12	0.07	0.13
MnO	0.06	0.04	0.03	0.04	0.05	0.06	0.02	0.04
P_2O_5	0.08	0.06	0.04	0.06	0.07	0.09	0.04	0.08
LOI	30.44	31.55	37.88	34.11	32.51	32.84	39.98	31.89
Sum	99.99	99.81	99.87	99.74	99.81	99.5	99.31	99.95
V (ppm)	18	17	19	20	18	20	18	18
Cr	20	20	10	14	20	100	10	20
Co	4.6	3.9	3.1	2.9	3.9	4.5	2.6	4.3
Ni	21	19	18	20	20	25	19	24
Rb	7.9	6.4	6.6	5.4	6.6	10.5	3.1	8.8
Ba	231.5	195.8	124.5	161.5	204.1	220.3	109.2	224.1
Sr	279.2	249.3	238.7	247.2	255.2	285.2	225.4	246.1
Th	6.87	7.82	7.89	7.45	7.98	7.13	6.95	7.54
U	0.93	0.74	0.41	0.61	0.78	0.62	0.38	0.84
Cu	25	20	15	20	21	25	14	22
Y	4.3	4.3	4.6	4.5	4.6	3.6	4.0	4.5
Zr	34	37	35	38	38	32	37	35
Pb	6	6	6	6	6	5	6	6
Nb	3.9	3.2	1.8	2.8	3.4	5.1	1.8	3.8
Hf	1.4	1.2	1.1	1.2	1.4	1.1	1.2	1.4
La (ppm)	16.01	14.02	9.88	11.82	14.51	15.41	8.88	15.54
Ce	27.68	23.94	17.02	20.21	25.44	27.09	16.11	25.51
Pr	2.92	2.51	1.88	2.22	2.61	2.93	1.74	2.81
Nd	15.64	14.29	10.89	12.13	14.54	16.43	9.81	15.29
Sm	1.79	1.65	1.24	1.38	1.65	1.83	1.11	1.74
Eu	0.46	0.41	0.31	0.35	0.41	0.44	0.26	0.44
Gd	1.84	1.65	1.18	1.405	1.69	1.88	1.08	1.84
Tb	0.16	0.13	0.12	0.15	0.13	0.22	0.12	0.15
Dy	1.16	0.99	0.69	0.88	1.02	1.16	0.64	1.11
Ho	0.21	0.18	1.16	0.17	0.21	0.24	0.63	0.19
Er	0.64	0.56	0.41	0.49	0.59	0.67	0.38	0.61
Tm	0.08	0.09	0.07	0.07	0.07	0.12	0.06	0.07
Yb	0.55	0.47	0.35	0.43	0.51	0.63	0.32	0.53
Lu	0.06	0.08	0.08	0.06	0.06	0.12	0.06	0.06
REE	70.51	60.99	46.1	54.39	63.11	75.86	42.34	68.22
Eu/Eu*	1.16	1.18	1.22	1.18	1.19	1.11	1.14	1.16
Ce/Ce*	0.94	0.94	0.93	0.92	0.94	0.92	0.92	0.89
Er/Nd	0.04	0.04	0.04	0.04	0.04	0.04	0.04	0.04
Y/Ho	20.24	23.61	3.99	26.47	22.02	15.10	6.35	23.68

Table 1. (Continued.)

	R-9	R-10	R-11	R-12	R-13	R-14	R-15
SiO_2 (wt.%)	12.45	13.91	13.81	25.82	17.35	18.85	12.87
Al_2O_3	4.98	4.98	5.52	9.33	6.62	7.54	5.15
Fe_2O_3	1.81	2.71	1.69	1.51	1.45	1.58	1.65
CaO	42.25	42.79	42.01	41.52	41.92	41.09	40.61
MgO	0.79	0.82	0.78	0.78	0.77	0.74	0.78
Na_2O	0.07	0.07	0.11	0.17	0.14	0.22	0.27
K_2O	0.47	0.99	0.76	0.34	0.29	0.35	0.39
TiO_2	0.07	0.09	0.12	0.29	0.16	0.18	0.07
MnO	0.02	0.04	0.04	0.04	0.04	0.04	0.02
P_2O_5	0.04	0.07	0.06	0.18	0.11	0.12	0.03
LOI	38.85	34.62	33.08	19.91	31.14	29.39	37.89
Sum	99.74	99.28	99.68	99.37	99.71	99.71	99.48
V (ppm)	17	17	18	41	24	35	17
Cr	10	10	20	60	70	40	10
Co	2.9	3.2	3.2	6.9	4.4	5	2.2
Ni	18	18	22	35	28	27	18
Rb	2.4	6.2	8.5	22.1	9.7	12.7	3.1
Ba	100.3	160.2	215.4	156.8	170.9	123.5	91.5
Sr	228.2	246.3	242.9	249.5	251.4	247.2	231.5
Th	8.21	7.84	9.67	11.32	9.21	12.74	14.06
U	0.33	0.54	0.81	0.45	0.41	0.33	0.31
Cu	13	15	22	45	27	30	13
Y	3.9	4.3	7.6	8.0	7.3	8.3	8.6
Zr	38	38	47	51	45	53	56
Pb	6	7	6	5	6	6	6
Nb	1.9	2.1	3.6	7.9	5.4	5.9	1.8
Hf	1.2	1.2	2.4	2.3	2.4	2.6	3.2
La (ppm)	8.27	12.09	15.11	115.11	38.36	9.85	7.64
Ce	15.28	20.51	28.69	147.1	64.15	20.87	16.63
Pr	1.64	2.18	2.74	2.22	2.38	1.86	1.52
Nd	9.24	13.14	14.98	12.51	13.28	10.34	8.63
Sm	1.05	1.49	1.71	1.37	1.45	1.16	0.97
Eu	0.26	0.34	0.54	0.44	0.46	0.41	0.35
Gd	1.02	1.41	1.76	1.42	1.54	1.21	0.97
Tb	0.14	0.12	0.16	0.21	0.21	0.18	0.14
Dy	0.63	0.81	1.08	0.91	0.98	0.75	0.61
Ho	0.39	0.17	0.21	0.21	0.23	0.18	0.14
Er	0.34	0.46	0.61	0.52	0.53	0.41	0.34
Tm	0.06	0.08	0.08	0.11	0.12	0.08	0.07
Yb	0.32	0.38	0.53	0.45	0.51	0.37	0.31
Lu	0.05	0.09	0.06	0.09	0.09	0.06	0.06
REE	40.36	51.68	66.14	160.78	87.35	99.13	38.28
Eu/Eu*	1.20	1.20	1.47	1.52	1.43	1.65	1.68
Ce/Ce*	0.96	0.92	1.03	1.05	1.03	1.13	1.16
Er/Nd	0.04	0.05	0.04	0.05	0.04	0.04	0.04
Y/Ho	9.94	25.00	36.31	38.10	31.52	45.83	61.61

Table 2. Pearson correlation coefficients among major, trace, and rare earth elements in the limestone at Kanigorgeh. The values of correlation coefficients below –0.85 and above 0.85 are shown in bold.

	Si	Al	Fe	Ca	Mg	Na	K	Ti	Mn	P	V	Cr	Co	Ni
Si	1.00													
Al	**0.97**	1.00												
Fe	–0.38	–0.38	1.00											
Ca	–0.36	–0.46	0.28	1.00										
Mg	–0.33	–0.40	0.53	0.46	1.00									
Na	0.36	0.44	–0.11	**–0.97**	–0.32	1.00								
K	–0.40	–0.37	0.68	0.52	0.26	–0.47	1.00							
Ti	**0.97**	**0.95**	–0.46	–0.32	–0.40	0.28	–0.36	1.00						
Mn	0.36	0.31	–0.34	0.35	0.05	–0.37	0.11	0.42	1.00					
P	**0.97**	**0.91**	–0.39	–0.25	–0.34	0.25	–0.40	**0.97**	0.45	1.00				
V	**0.90**	**0.90**	–0.33	–0.50	–0.36	0.51	–0.54	**0.88**	0.11	**0.89**	1.00			
Cr	0.59	0.47	–0.53	–0.06	–0.02	0.08	–0.64	0.55	0.53	0.66	0.48	1.00		
Co	**0.93**	**0.89**	–0.42	–0.14	–0.29	0.11	–0.31	**0.94**	0.55	**0.95**	0.80	0.63	1.00	
Ni	**0.92**	**0.86**	–0.55	–0.34	–0.42	0.31	–0.57	**0.93**	0.33	**0.95**	**0.87**	0.73	**0.89**	1.00
Rb	**0.95**	**0.90**	–0.36	–0.27	–0.24	0.27	–0.35	**0.95**	0.42	**0.96**	**0.88**	0.63	**0.94**	**0.93**
Ba	0.17	0.12	–0.29	0.49	–0.06	–0.54	0.34	0.27	0.85	0.25	–0.15	0.32	0.38	0.21
Sr	0.33	0.26	–0.42	0.30	0.15	–0.33	–0.07	0.36	**0.96**	0.40	0.08	0.63	0.52	0.32
Th	0.39	0.47	–0.18	**–0.98**	–0.41	**0.98**	–0.45	0.32	–0.33	0.27	0.52	0.07	0.15	0.34
U	–0.04	–0.05	–0.16	0.51	–0.06	–0.59	0.58	0.08	0.70	0.00	–0.34	–0.06	0.16	–0.07
Cu	**0.96**	**0.93**	–0.51	–0.28	–0.35	0.24	–0.41	**0.99**	0.48	**0.97**	**0.87**	0.64	**0.95**	**0.95**
Y	0.50	0.58	–0.29	**–0.91**	–0.48	**0.91**	–0.43	0.49	–0.19	0.42	0.60	0.17	0.28	0.52
Zr	0.43	0.52	–0.18	–0.95	–0.47	**0.95**	–0.42	0.39	–0.34	0.33	0.56	0.06	0.17	0.40
Pb	–0.55	–0.48	0.69	0.15	0.04	–0.07	0.67	–0.53	–0.27	–0.50	–0.50	–0.70	–0.57	–0.63
Nb	**0.94**	**0.89**	–0.56	–0.30	–0.40	0.27	–0.50	**0.95**	0.51	**0.96**	0.85	0.76	**0.94**	**0.97**
Hf	0.37	0.45	–0.34	**–0.94**	–0.51	**0.91**	–0.45	0.37	–0.21	0.30	0.45	0.15	0.16	0.41
Ce	**0.89**	0.83	–0.29	–0.28	–0.14	0.28	–0.37	**0.87**	0.15	0.84	0.77	0.49	0.79	0.85
Eu	0.48	0.49	–0.49	–0.13	–0.34	0.08	–0.01	0.56	0.69	0.51	0.25	0.48	0.54	0.54
REE	**0.98**	**0.94**	–0.41	–0.32	–0.33	0.30	–0.41	**0.99**	0.38	**0.98**	**0.91**	0.61	**0.95**	**0.96**

Table 2. (Continued.)

	Rb	Ba	Sr	Th	U	Cu	Y	Zr	Pb	Nb	Hf	Ce	Eu	REE
Si														
Al														
Fe														
Ca														
Mg														
Na														
K														
Ti														
Mn														
P														
V														
Cr														
Co														
Ni														
Rb	1.00													
Ba	0.27	1.00												
Sr	0.38	0.76	1.00											
Th	0.31	−0.47	−0.30	1.00										
U	0.03	**0.92**	0.57	−0.51	1.00									
Cu	**0.97**	0.32	0.44	0.28	0.10	1.00								
Y	0.46	−0.27	−0.22	**0.91**	−0.36	0.46	1.00							
Zr	0.35	−0.44	−0.36	**0.96**	−0.48	0.34	**0.96**	1.00						
Pb	−0.59	−0.17	−0.38	−0.13	0.03	−0.62	−0.15	−0.08	1.00					
Nb	**0.94**	0.33	0.48	0.31	0.06	**0.97**	0.47	0.35	−0.63	1.00				
Hf	0.32	−0.26	−0.20	**0.92**	−0.34	0.33	**0.97**	**0.95**	−0.12	0.37	1.00			
Ce	**0.86**	0.08	0.14	0.28	−0.10	0.85	0.44	0.38	−0.56	0.78	0.33	1.00		
Eu	0.56	0.77	0.59	0.13	0.61	0.60	0.39	0.19	−0.29	0.64	0.37	0.36	1.00	
REE	**0.98**	0.22	0.34	0.33	0.00	**0.99**	0.49	0.39	−0.59	**0.96**	0.36	**0.89**	0.53	1.00

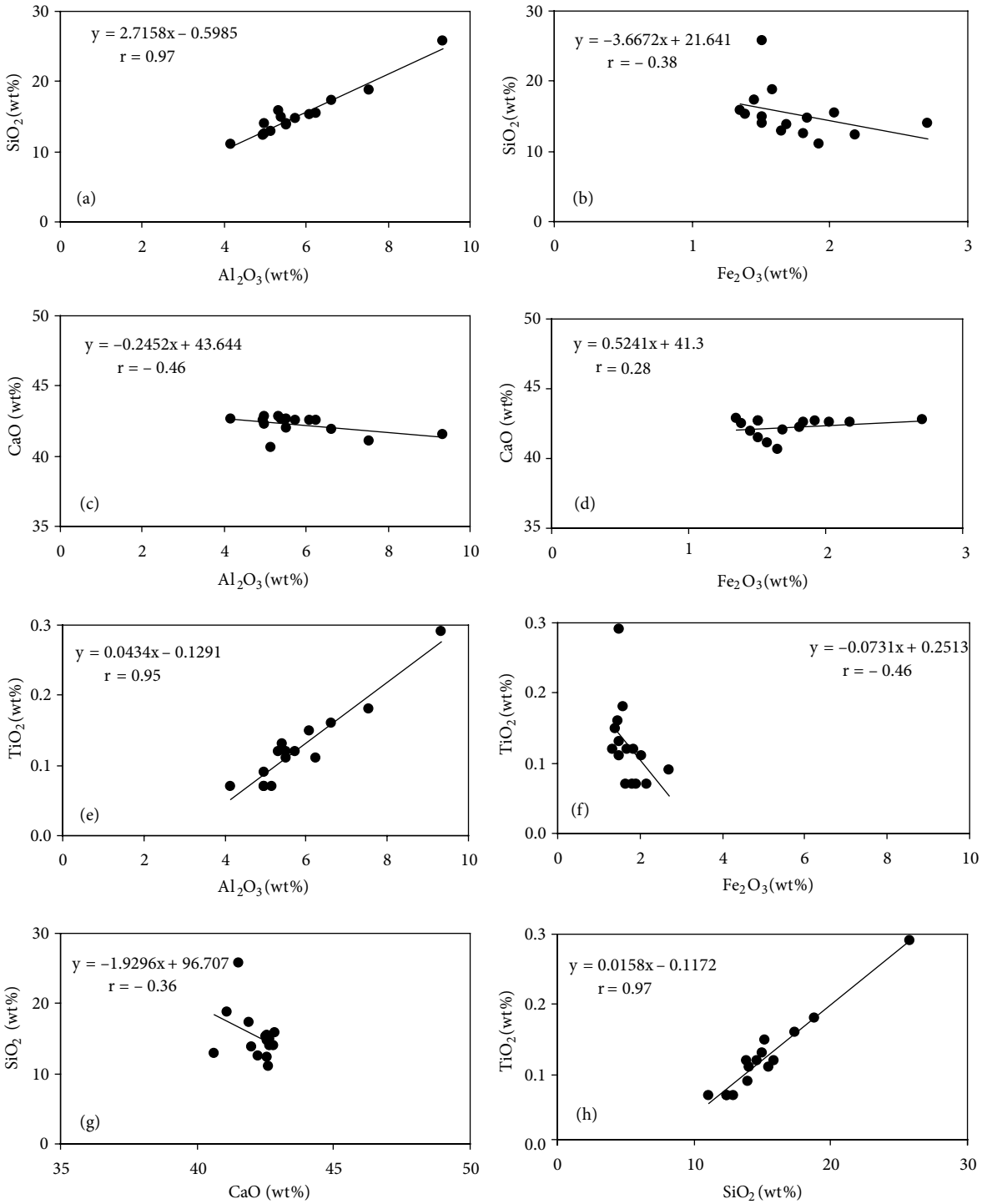

Figure 4. Bivariate plots for pairs of Al_2O_3–SiO_2 **(a)**, Fe_2O_3 – SiO_2 **(b)**, Al_2O_3 – CaO **(c)**, Fe_2O_3 – CaO **(d)**, Al_2O_3 – TiO_2 **(e)**, Fe_2O_3 – TiO_2 **(f)**, SiO_2 – CaO **(g)**, and SiO_2 – TiO_2 in the limestone at Kanigorgeh.

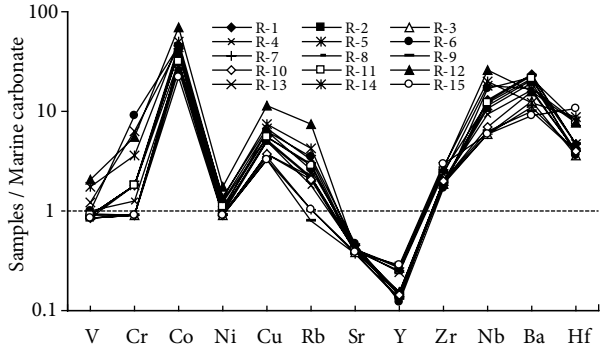

Figure 5. Distribution patterns of trace elements normalized to marine carbonate (Turekian and Wedepohl, 1961) for samples from the limestone at Kanigorgeh.

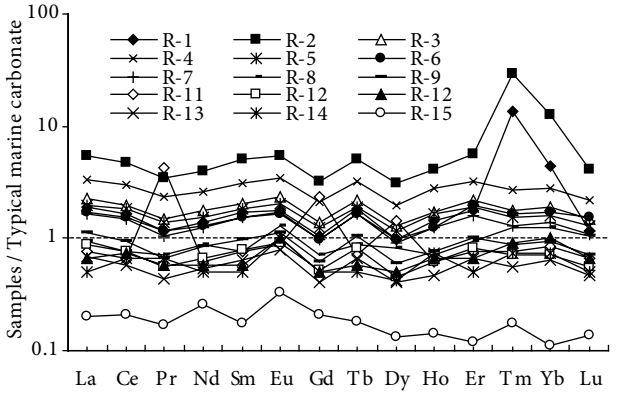

Figure 6. Distribution patterns of REEs normalized to typical marine carbonate (Bellanca et al., 1997) for samples from the limestone at Kanigorgeh.

in the limestone at Kanigorgeh shows that the REEs have a positive correlations with SiO_2 (r = 0.98; Figure 7c), TiO_2 (r = 0.99; Figure 7d), V (r = 0.91; Figure 7e), Co (r = 0.95; Figure 7f), Ni (r = 0.96; Figure 7g), Rb (r = 0.98), Cu (r = 0.99; Figure 7h), and Nb (r = 0.96; Figure 7i), and negative correlation with CaO (r = –0.32; Figure 7j). These relations clearly provide firm reasons to attribute a terrigenous origin to REEs in the limestone.

5.2. Ce anomaly

The anomaly values of Ce (i.e. Ce/Ce*) in the limestone at Kanigorgeh show a narrow range of 0.89–1.16 (with an average 0.98). The value for marine waters ranges from <0.1 to 0.4 (Elderfield and Greave, 1982). The mean value in shales is about 1 (Piepgras and Jacobsen, 1992; Madhavaraju and Lee, 2009). Therefore, it appears that the Ce/Ce* values in the limestone are influenced by the relative proportions of precipitates derived from both pure seawater (carbonates) and fluvial suspension materials (clastic contaminations) (Murray et al., 1991a). Commonly, the positive anomaly of Ce is generated as a result of terrigenous input (Nath et al., 1992; Madhavaraju and Ramasamy, 1999; Armstrong-Altrin et al., 2003). In addition, factors like paleo-redox (Liu et al., 1988; German and Elderfield, 1990; Armstrong-Altrin et al., 2003), fluviatile colloids enriched by Fe-organics (Sholkovitz, 1992), and scavenging processes (Masuzawa and Koyama, 1989) could play crucial roles in the occurrence of positive Ce anomalies. The Ce/Ce* values display negative correlation with U (r = –0.5; Figure 8a) and CaO (r = –0.98; Figure 8b), indicating that the variations in Ce anomalies are not related to the paleo-redox conditions of the depositional environment. The Ce/Ce* values also have negative correlations with reactive scavenging-type particles like Pb, Mn, and Fe (r = –0.14 to –0.27; Figures 8c–8e). These correlations show that the studied limestone was precipitated in a shallow marine environment wherein the role of scavenging processes is comparatively more trivial than that of deep marine environments. Ce has positive correlations with elements such as Al (r = 0.83), Ti (r = 0.87), V (r = 0.77), Co (r = 0.79), Ni (r = 0.85), Rb (r = 0.86), Cu (r = 0.85), and Nb (r = 0.78) in the studied limestone (Table 2). The Ce/Ce* values strongly and positively correlate with Si (r = 0.96), Zr (r = 0.96; Figure 8f), Hf (r = 0.95), and Y (r = 0.93). What can be inferred from these correlations is that Ce abundances and Ce anomaly variations in the studied limestone were controlled by detrital input.

5.3. Eu anomaly

Eu anomaly values can provide great help in comprehending the physicochemical conditions of various geochemical systems such as the depositional environment of limestones (Derry and Jacobsen, 1990). The result of calculations for Eu anomalies in the limestone at Kanigorgeh demonstrates positive anomalies ranging from 1.11 to 1.68, with a mean of 1.30. Commonly positive Eu anomalies (normalized to PAAS) are observed in limestones influenced by hydrothermal processes (Siby et al., 2008; Madhavaraju and Lee, 2009). In addition, intense diagenesis (Murray et al., 1991a; Nath et al., 1992), variations in quantity of feldspars (Nath et al., 1992), and aeolian input (Elderfield, 1988) are other factors that can create positive Eu anomalies in limestones. Because of negative correlations between Ce/Ce* and components like Fe_2O_3 and MnO (see Section 5.2), the role of hydrothermal activities in the occurrence of positive Eu anomalies in the limestone at Kanigorgeh may be ruled out. No aeolian materials in the limestone of the Ruteh Formation have been reported so far. The role of diagenetic processes in the occurrence of positive Eu anomalies in the limestone can be postulated by positive correlations between Eu/Eu* and certain immobile elements such as Zr, Y, Th, and Hf (Madhavaraju and Lee, 2009). The strong and positive correlations among pairs Eu/Eu* – Zr (r = 0.98; Figure 9a), Eu/Eu* – Y (r =

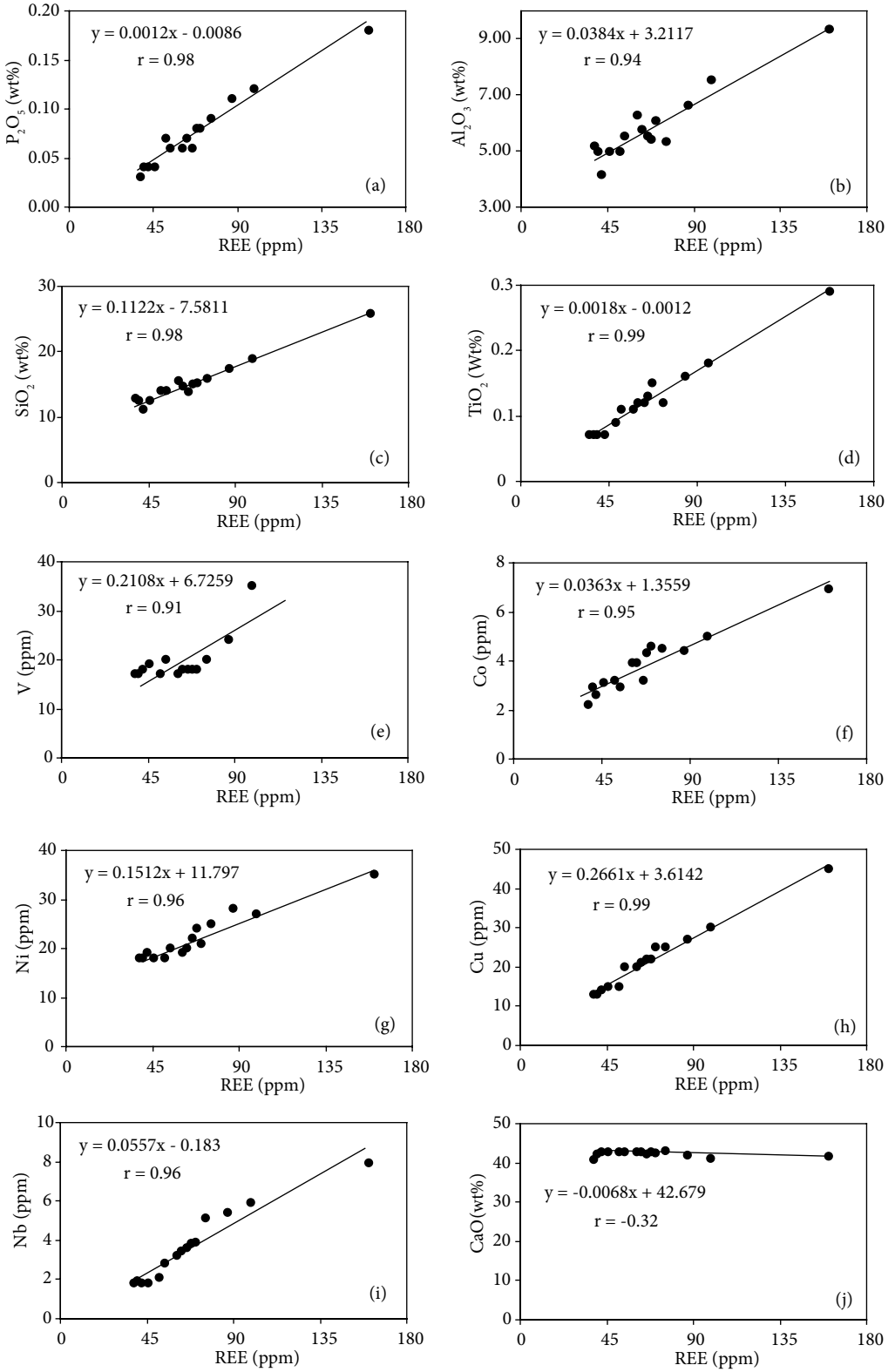

Figure 7. Bivariate plots for pairs of REEs – P_2O_5 **(a)**, REEs – Al_2O_3 **(b)**, REEs – SiO_2 **(c)**, REEs – TiO_2 **(d)**, REEs – V **(e)**, REEs – Co **(f)**, REEs – Ni **(g)**, REEs – Cu **(h)**, REEs – Nb **(i)**, and REEs – CaO **(j)** in the limestone at Kanigorgeh.

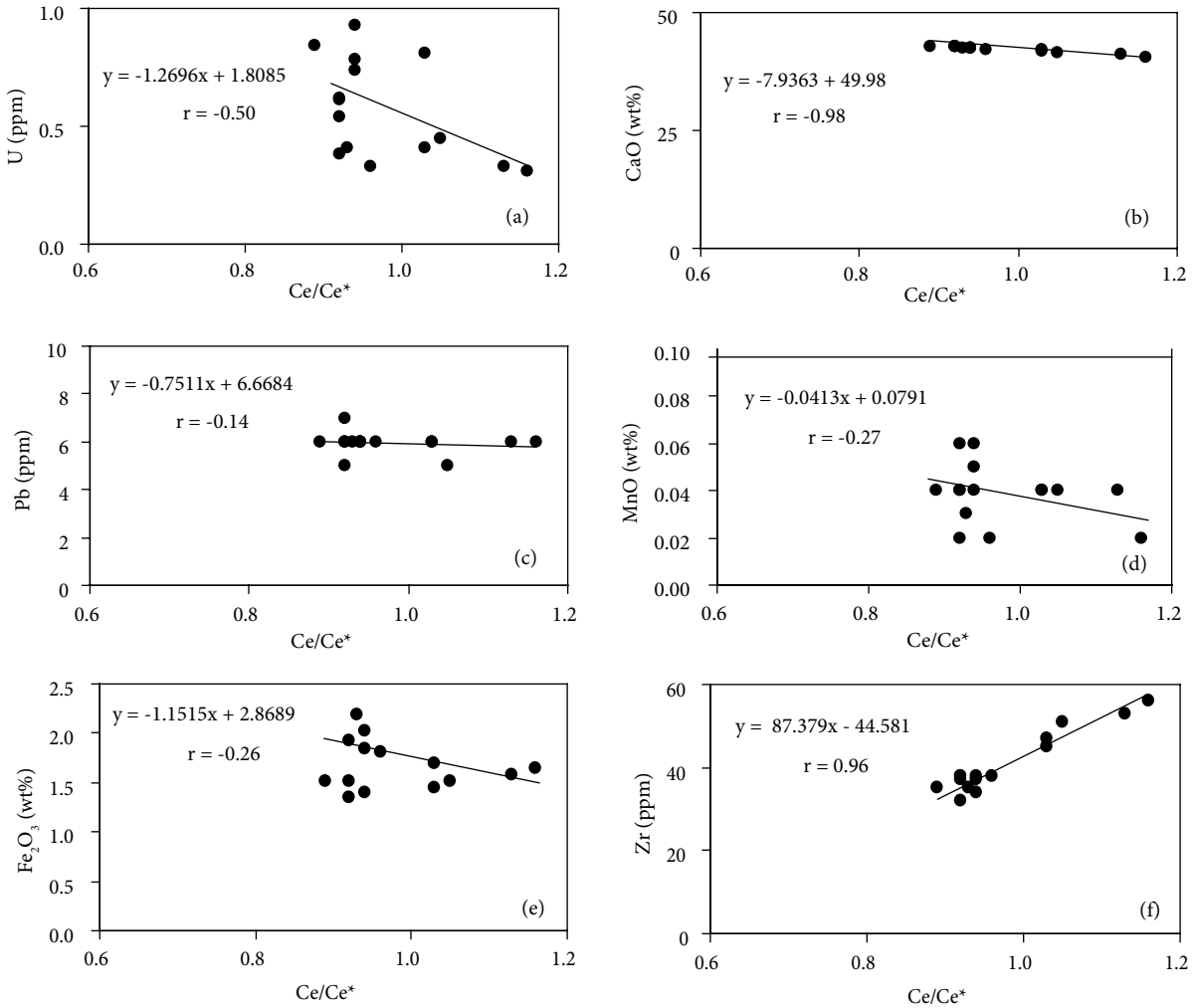

Figure 8. Bivariate plots for pairs of Ce/Ce* – U **(a)**, Ce/Ce* – CaO **(b)**, Ce/Ce* – Pb **(c)**, Ce/Ce* – MnO **(d)**, Ce/Ce* – Fe_2O_3 **(e)**, and Ce/Ce* – Zr **(f)** in the limestone at Kanigorgeh.

0.99; Figure 9b), Eu/Eu* – Th (r = 0.98; Figure 9c), and Eu/Eu* – Hf (r = 0.96; Figure 9d) advocate the effective role of diagenesis in the occurrence of Eu anomalies in the studied limestone. Furthermore, the effect of diagenetic alteration in the limestone can be deduced by the strongly positive correlation between the pair of Mn – Sr (r = 0.96) (Brand and Veizer, 1980). Inclusions of detrital feldspars in sediments can bring about positive Eu anomalies in limestones (Murray et al., 1991a). The ratios of oxides like Na_2O/Al_2O_3 and K_2O/Al_2O_3 can help in recognition of different kinds of feldspars in sediments (Madhavaraju and Lee, 2009; Nagarajan et al., 2011). The limestone at Kanigorgeh show strong and positive correlations between Na_2O/Al_2O_3 and Eu/Eu* (r = 0.87; Figure 10a) but negative correlation between K_2O/Al_2O_3 and Eu/Eu* (r = –0.50; Figure 10b). Therefore, it seems that in addition to diagenetic processes, the presence of plagioclase in the studied limestone also played a significant role in the occurrence of positive Eu anomalies.

5.4. Ratios of Y/Ho and Er/Nd in the limestone

Yttrium has identical charge and ionic radius with Ho and Dy. Therefore, yttrium in distribution patterns of REEs is inserted between Ho and Dy (Bau, 1996). Although Y and Ho have similar geochemical behavior, Ho can be removed from seawater twice as fast as Y. This phenomenon is related to the difference in degree of surface complex stabilities, which leads to a notable superchondritic marine ratio of Y/Ho (Bau, 1996; Nozaki et al., 1997). Terrigenous materials and volcanic ashes have constant chondritic values of Y/Ho (approximately 28). Seawaters have Y/Ho values greater than those of volcanic ashes, ranging from 44 to 74 (Bau, 1996; Nozaki et al., 1997). In this study, the limestone at Kanigorgeh has Y/Ho values varying noticeably from 3.99 to 61.61 (with a mean of

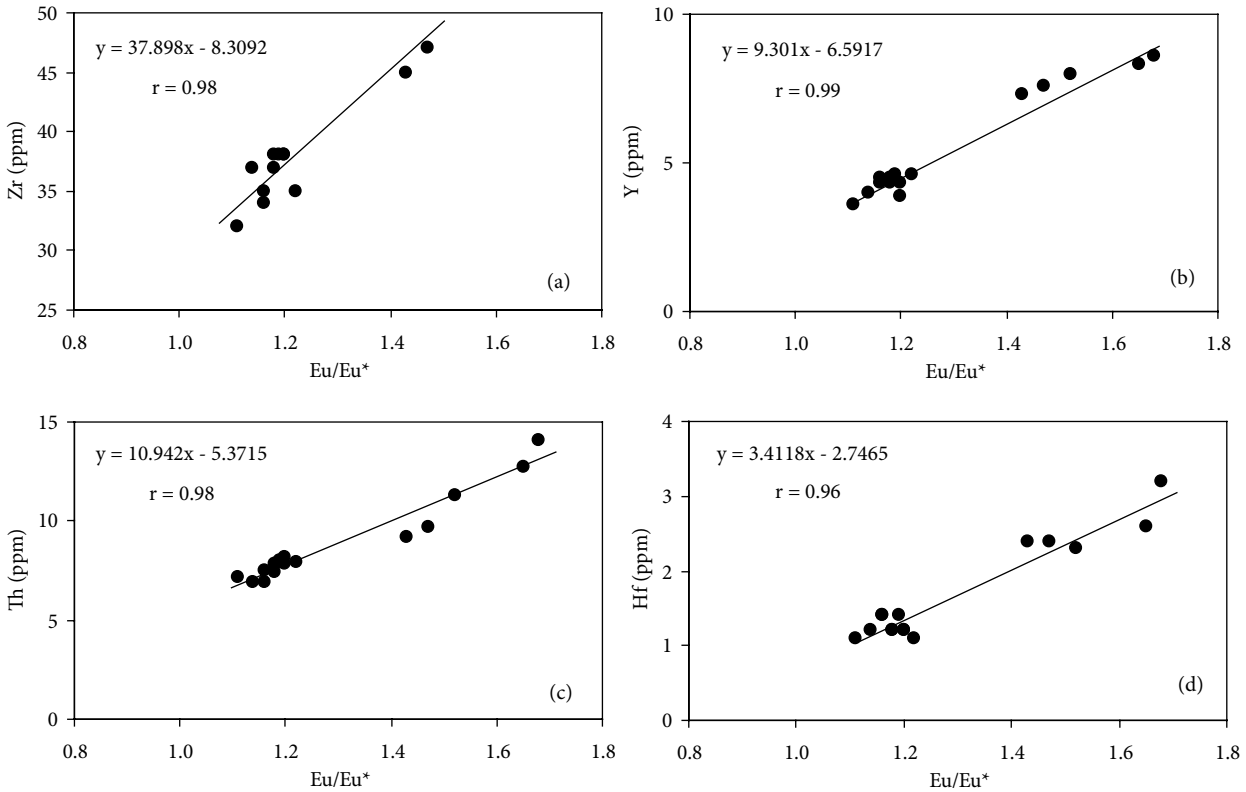

Figure 9. Bivariate plots for pairs of Eu/Eu* – Zr **(a)**, Eu/Eu* – Y **(b)**, Eu/Eu* – Th **(c)**, and Eu/Eu* – Hf **(d)** in the limestone at Kanigorgeh.

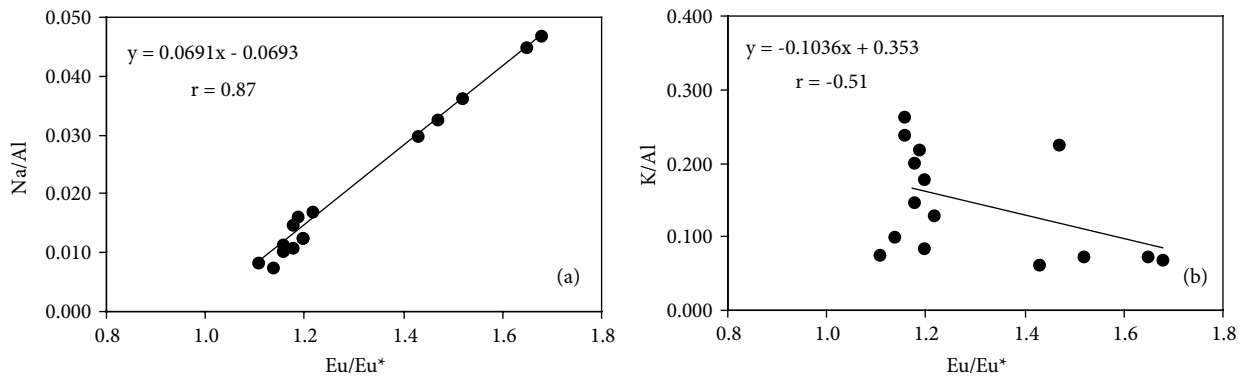

Figure 10. Bivariate plots for pairs of Eu/Eu* – Na_2O/Al_2O_3 **(a)** and Eu/Eu* – K_2O/Al_2O_3 **(b)** in the limestone at Kanigorgeh.

25.98). These values may indicate that the limestone likely suffered terrigenous contamination. The value of Er/Nd in normal seawater is ~0.27 (De Baar et al., 1988). The Er/Nd value in limestones can efficiently reveal the seawater signature kept by the marine carbonates. Both detrital materials and diagenetic processes can cause preferential concentration of Nd relative to Er and also can reduce the Er/Nd values to <0.1 (German and Elderfield, 1990; Bellanca et al., 1997). The Er/Nd values in the studied limestone display a narrow range of 0.04–0.05, which in turn indicates the effective role of detrital materials and diagenetic processes in the distribution of Er and Nd in the limestone at Kanigorgeh. Additionally, the controlling role of diagenetic processes in the distribution of REEs in limestones can be established by an excellent positive correlation between Eu/Eu* and Ce/Ce* (Song et al., 2014). The existence of strong and positive correlation between Eu/Eu* and Ce/Ce* (r = 0.98; Figure 11) in the limestone

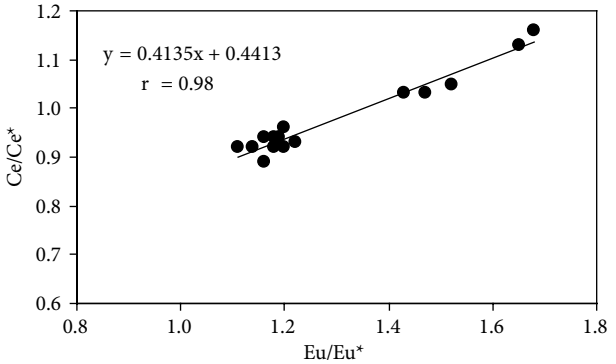

Figure 11. A bivariate plot for pair of Eu/Eu* – Ce/Ce* in the limestone at Kanigorgeh.

demonstrates that the diagenesis was a key controlling factor in the distribution of REEs at Kanigorgeh.

5.5. The limestone role in supplying REEs for the bauxites

The distribution pattern of REEs in weathered materials and residual ores has been accepted as an important marker for determination and recognition of parent rocks by many researchers (Mongelli, 1997; Calagari and Abedini, 2007; Mameli et al., 2007; Karadağ et al., 2009). In addition, Eu anomaly can be used as a conservative elemental index in weathered environments for determination of parental affinity for bauxite ores (Mongelli, 1997; Mameli et al., 2007; Mongelli et al., 2014). By noting these explanations, in this study the distribution patterns of REEs along with Eu anomaly in the bauxitic ores and the host limestone were compared to determine the potential role of the latter in supplying REEs for the former.

The distribution pattern of REEs normalized to chondrite (Taylor and McLennan, 1985) for the bauxitic ores (data from Abedini and Calagari, 2014) (Figure 12a) and the host limestone (Figure 12b) delineate totally different aspects. Comparison of these two patterns indicates that the differentiation degree of LREEs (La-Eu) from HREEs (Gd-Lu) in samples of the limestone is more pronounced than that of the bauxitic ores. That is, while the discrepancies in the concentration degree of REEs of the bauxitic ores are far greater than that of the limestone (Figures 12a and 12b). The outstanding key point that can be inferred from comparison of distribution pattern of REEs in two types of rocks is that the negative Eu anomaly values of the bauxitic ores are far greater than that of the limestone. The existence of such eminent discrepancies indicates the inconsequential role of the host limestone in providing REEs for the bauxitic ores. It seems that REEs of the bauxitic ores, analogous to major constituents, were also derived chiefly from basaltic rocks.

6. Conclusions

The most important results obtained from geochemical considerations on the limestone of the Ruteh Formation in the Kanigorgeh mining district are as follows:

1) Geochemical indications such as low ratio of Y/Ho and high values of REEs show that the concentration of REEs in the studied limestone is associated with incorporation of terrigenous materials. This premise can be further supported by strongly positive correlation of REEs with elements such as Si, Al, Ti, V, Co, Ni, Rb, Cu, and Nb, and by negative correlation between REEs and CaO.

2) The strong and positive correlations between Ce/Ce* and elements like Si, Al, Zr, Hf, and Y along with negative correlations between Ce/Ce* and certain components such as CaO, U, Fe_2O_3, and MnO reveal that variation in values of Ce anomalies in the limestone were substantially controlled by fluvial detrital input. Furthermore, the mentioned negative correlations furnish a strong reason for deposition of the limestone in a shallow marine environment.

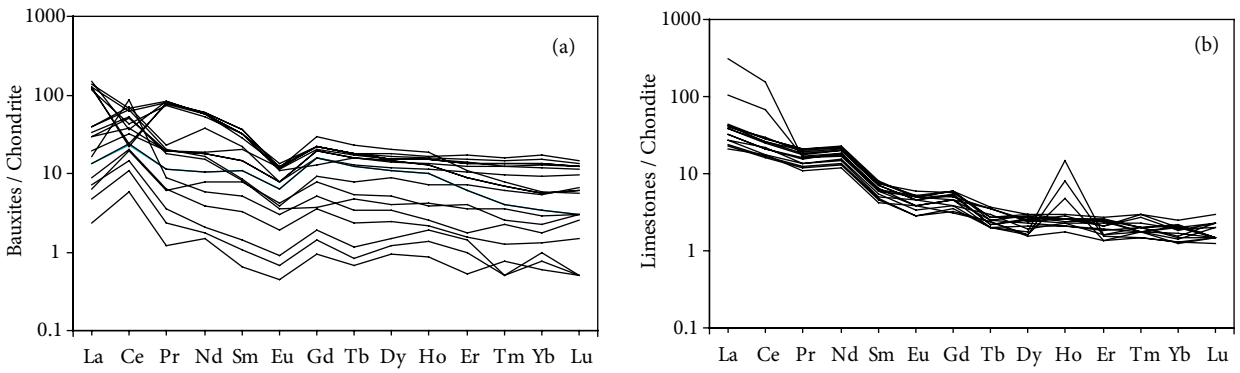

Figure 12. The chondrite-normalized REE patterns for **(a)** the bauxite ores (data from Abedini and Calagari, 2014) and **(b)** the limestone at Kanigorgeh.

3) The positive correlations between Eu/Eu* and elements such as Zr, Y, Th, and Hf along with strongly positive correlation between pairs of Na_2O/Al_2O_3–Eu/Eu* and REEs – P_2O_5 provided compelling evidence that made us conclude that the positive Eu anomalies in the limestone at Kanigorgeh occurred as the result of functions of diagenetic processes and existence of detrital plagioclase.

4) The low Er/Nd values along with strongly positive correlation between Eu/Eu* and Ce/Ce* indicate the effective role of diagenetic fluids in the concentration of REEs in the limestone.

5) The conspicuous differences like the distribution patterns of REEs and Eu anomaly values between the limestone and the bauxitic ores demonstrate that the former could not play a significant role in supplying REEs for the latter.

Acknowledgments

This work was supported financially by the Research Bureau of Urmia University. We would like to express thanks and gratitude to the authorities of this bureau. Our gratitude is further expressed to Dr Fuat Yavuz, Dr Nurullah Hanilçi, and two anonymous reviewers for reviewing the manuscript and making critical comments and valuable suggestions.

References

Abedini A, Calagari AA (2013a). Rare earth elements geochemistry of Sheikh-Marut laterite deposit, NW Mahabad, West-Azarbaidjan province, Iran. Acta Geol Sin-Engl 87: 176–185.

Abedini A, Calagari AA (2013b). Geochemical characteristics of bauxites: the Permian Shahindezh horizon, NW Iran. N J Geol Palaont Abh 270: 301–324.

Abedini A, Calagari AA (2013c). Geochemical characteristics of Kanigorgeh ferruginous bauxite horizon, West-Azarbaidjan province, NW Iran. Period Mineral 82: 1–23.

Abedini A, Calagari AA (2014). REE geochemical characteristics of titanium-rich bauxites: the Permian Kanigorgeh horizon, NW Iran. Turkish J Earth Sci 23: 513–532.

Aghanabati A (2004). Geology of Iran. Tehran, Iran: Geological Survey of Iran (in Persian).

Armstrong-Altrin JS, Verma SP, Madhavaraju J, Lee YI, Ramasamy S (2003). Geochemistry of Late Miocene Kudankulam Limestones, South India. Int Geol Rev 45: 16–26.

Bau M (1996). Controls on fractionation of isovalent trace elements in magmatic and aqueous systems: Evidence from Y/Ho, Zr/Hf and lanthanide tetrad effect. Contrib Mineral Petr 123: 323–333.

Bau M, Koschinsky A, Dulski P, Hein JR (1996). Comparison of the partitioning behaviours of yttrium, rare earth elements, and titanium between hydrogenetic marine ferromanganese crusts and seawater. Geochim Cosmochim Ac 60: 1709–1725.

Bellanca A, Masetti D, Neri R (1997). Rare earth elements in limestone/marlstone couplets from the Albian-Cenomanian Cismon section (Venetian region, northern Italy): assessing REE sensitivity to environmental changes. Chem Geol 141: 141–152.

Brand U, Veizer J (1980). Chemical diagenesis of a multi component carbonate system: trace elements. J Sediment Petr 50: 1219–1236.

Byrne RH, Liu X, Schijf J (1996). The influence of phosphate coprecipitation on rare earth element distributions in natural waters. Geochim Cosmochim Ac 60: 3341–3346.

Calagari AA, Abedini A (2007). Geochemical investigations on Permo–Triassic bauxite deposit at Kanisheeteh, east of Bukan, Iran. J Geochem Explor 94: 1–18.

Calagari AA, Kangrani F, Abedini A (2010). Geochemistry of minor, trace and rare earth elements in Biglar Permo-Triassic bauxite deposit, northwest of Abgarm, Ghazvin Province, Iran. J Sci Islamic Repub Iran 21: 225–236.

Calagari AA, Kangrani F, Abedini A (2015). Geochemical characteristics of a laterite: the Jurassic Zan deposit, Iran. Acta Geodyn Geomater 12: 67–77.

De Baar HJW, German CG, Elderfield H, Van-Gaans P (1988). Rare earth elements distributions in anoxic waters of the Cariaco Trench. Geochim Cosmochim Ac 52: 1203–1219.

Derry LA, Jacobsen SB (1990). The chemical evolution of Precambrian seawater: evidence from REEs in banded iron formations. Geochim Cosmochim Ac 54: 2965–2977.

Elderfield H (1988). The oceanic chemistry of the rare earth elements. Philos T Roy Soc A 325: 105–126.

Elderfield H, Greaves MJ (1982). The rare earth elements in seawater. Nature 296: 214–219.

Elderfield H, Upstill-Goddard R, Sholkovitz ER (1990). The rare earth elements in rivers, estuaries, and coastal seas and their significance to the composition of ocean waters. Geochim Cosmochim Ac 54: 971–991.

German CR, Elderfield H (1990). Application of Ce anomaly as a paleo-redox indicator: the ground rules. Paleoceanography 5: 823–833.

Greaves MJ, Elderfield H, Sholkovitz ER (1999). Aeolian sources of rare earth elements to the Western Pacific Ocean. Mar Chem 68: 31–38.

Hanilçi N (2013). Geological and geochemical evolution of the Bolkardağı bauxite deposits, Karaman-Turkey: transformation from shale to bauxite. J Geochem Explor 133: 118–137.

Kamineni DC, Efthekhar-Nezad J (1977). Mineralogy of the Permian laterite of Northwestern Iran. Tscher Miner Petrog 24: 195–204.

Karadağ M, Kupeli S, Aryk F, Ayhan A, Zedef V, Doyen A (2009). Rare earth element (REE) geochemistry and genetic implications of the Mortaş bauxite deposit (Seydişehir/Konya–Southern Turkey). Chemie Erde-Geochem 69: 143–159.

Liu YG, Miah MRU, Schmitt RA (1988). Cerium: a chemical tracer for paleooceanic redox conditions. Geochimica Cosmochim Ac 52: 1361–1371.

Liu X, Wang Q, Deng J, Zhang Q, Sun S, Meng J (2010). Mineralogical and geochemical investigations of the Dajia Salento-type bauxite deposits, western Guangxi, China. J Geochem Explor 105: 137–152.

Madhavaraju J, González-León CM (2012). Depositional conditions and source of rare earth elements in carbonate strata of the Aptian-Albian Mural Formation, Pitaycachi section, northeastern Sonora, Mexico. Revista Mexicana de Ciencias Geológicas 29: 478–491.

Madhavaraju J, González-León CM, Lee YI, Armstrong-Altrin, JS, Reyes-Campero LM (2010). Geochemistry of the Mural Formation (Aptian-Albian) of the Bisbee Group, Northern Sonora, Mexico. Cretaceous Res 31: 400–414.

Madhavaraju J, Lee Y (2009). Geochemistry of the Dalmiapuram Formation of the Uttatur Group (Early Cretaceous), Cauvery basin, southeastern India: implications on provenance and paleo-redox conditions. Revista Mexicana de Ciencias Geológicas 26: 380–394.

Madhavaraju J, Ramasamy S (1999). Rare earth elements in limestones of Kallankurichchi Formation of Ariyalur Group, Tiruchirapalli Cretaceous, Tamil Nadu. J Geol Soc India 54: 291–301.

Mameli P, Mongelli G, Oggiano G, Dinelli E (2007). Geological, geochemical and mineralogical features of some bauxite deposits from Nurra (western Sardinia, Italy): insights on conditions of formation and parental affinity. Int J Earth Sci 96: 887–902.

Masuzawa, T, Koyama M (1989). Settling particles with positive Ce anomalies from the Japan Sea. Geophys Res Lett 16: 503–506.

McLennan SM (1989). Rare earth elements in sedimentary rocks: Influence of provenance and sedimentary processes. In: Lipin BR, McKay GA, editors. Geochemistry and Mineralogy of Rare Earth Elements. Chantilly, VA, USA: Mineralogical Society of America, pp. 169–200.

Mongelli G (1997). Ce-anomalies in the textural components of Upper Cretaceous karst bauxites from the Apulian carbonate platform (southern Italy). Chem Geol 140: 69–79.

Mongelli G, Boni M, Buccione R, Sinisi R (2014). Geochemistry of the Apulian karst bauxites (southern Italy): chemical fractionation and parental affinities. Ore Geol Rev 63: 9–21.

Murphy K, Dymond J (1984). Rare earth element fluxes and geochemical budget in the eastern equatorial Pacific. Nature 307: 444–447.

Murray RW, Ten Brink MRB, Brumsack HJ, Gerlach DC, Russ GP 3rd (1991a). Rare earth elements in Japan Sea sediments and diagenetic behaviour of Ce/Ce*: results from ODP Leg 127. Geochim Cosmochim Ac 55: 2453–2466.

Murray RW, Ten Brink MRB, Gerlach DC, Russ GP 3rd, Jones DL (1991b). Rare earth, major and trace elements in chert from the Franciscan complex and Monterey Group, California: assessing REE sources to fine grained marine sediments. Geochim Cosmochim Ac 55: 1875–1895.

Nagarajan R, Madhavaraju J, Armstrong-Altrin JS, Nagendra R (2011). Geochemistry of Neoproterozoic limestones of the Shahabad Formation, Bhima Basin, Karnataka, southern India. Geosci J 15: 9–25.

Nagendra R, Nagarajan R, Bakkiaraj D, Armstrong-Altrin JS (2011). Depositional and post-depositional setting of Maastrichtian limestone, Ariyalur Group, Cauvery Basin, South India: a geochemical appraisal. Carbonates Evaporites 26: 127–147.

Nath BN, Roelandts I, Sudhakar M, Plueger WL (1992). Rare earth element patterns of the Central Indian Basin sediments related to their lithology. Geophys Res Lett 19: 1197–1200.

Nothdurft LD, Webb GE, Kamber BS (2004). Rare earth element geochemistry of Late Devonian reefal carbonates, Canning Basin, Western Australia: confirmation of a seawater REE proxy in ancient limestone. Geochim Cosmochim Ac 68: 263–283.

Nozaki Y, Zhang J, Amakawa H (1997). The fractionation between Y and Ho in the marine environment. Earth Planet Sci Lett 148: 329–340.

Piepgras DJ, Jacobsen SB (1992). The behaviour of rare earth elements in seawater: precise determination of variations in the North Pacific water column. Geochim Cosmochim Ac 56: 1851–1862.

Piper DZ (1974). Rare earth elements in the sedimentary cycle: a summary. Chem Geol 14: 285–304.

Rollinson HU (1993). Using Geochemical Data: Evaluation, Presentation, Interpretation. London, UK: Longman Scientific and Technical.

Sholkovitz ER (1992). Chemical evolution of rare earth elements: fractionation between colloidal and solution phases of filtered river water. Earth Planet Sci Lett 114: 77–84.

Siby K, Nath BN, Ramaswamy V, Naman D, Gnaneshwar R, Kamesh Raju KA, Selvaraj K, Chen CTA (2008). Possible, detrital, diagenetic and hydrothermal sources for Holocene sediments of the Andaman back arc basin. Mar Geol 247: 178–193.

Song C, Herong G, Linhua S (2014). Geochemical characteristics of REE in the Late Neo-Proterozoic limestone from northern Anhui Province, China. Chin J Geochem 33: 187–193.

Taylor Y, McLennan SM (1985). The Continental Crust: Its Composition and Evolution. 1st ed. Oxford, UK: Blackwell.

Toyoda D, Nakamura Y, Masuda A (1990). Rare earth elements of Pacific pelagic sediments. Geochim Cosmochim Ac 54: 1093–1103.

Turekian KK, Wedepohl KH (1961). Distribution of elements in some major units of earth's crust. Geol Soc Am Bull 72: 175–192.

Veizer J (1983). Trace elements and isotopes in sedimentary carbonates. In: Reeder RJ, editor. Carbonates: Mineralogy and Chemistry, Vol. 11. Chantilly, VA, USA: Mineralogical Society of America, pp. 265–299.